

Synthesis and characterization of Fe₃O₄@Ag core-shell: structural, morphological, and magnetic properties

Mahdi Ghazanfari, Fatemeh Johar, Ahmad Yazdani *

Department of Basic Sciences, Tarbiat Modares University (TMU), P.O. Box 14115-175, Tehran, Iran

Received 29 June 2014; Accepted 30 December 2014

* Corresponding author: yazdania@modares.ac.ir ; Tel: +98 21 82883439

Abstract

This paper is a report on the synthesis of the Fe₃O₄@Ag core-shell with high saturation magnetization of magnetite nanoparticles as the core, by using polyol route and silver shell by chemical reduction. X-ray diffraction (XRD) and Fourier transform infrared spectroscopy analyses confirmed that the particles so produced were monophasic. The magnetic properties of the product were investigated by using a vibrating sample magnetometer. Magnetic saturation of magnetite was 91 emu/g that around about bulk magnetization. This high saturation magnetization can be attributed to the thin dead layer. By using polyethylene glycol as a surfactant to separate and restrict the growth of the particles, magnetostatic interactions are in good agreement with the remanence ratio analysis. Morphology and the average size of the particles were determined with field emission scanning electron microscope (FESEM). Spherical aggregates of Fe₃O₄ (size around 73 nm) are composed of a small primary particle size of about 16 nm. Silver deposition was done using butylamine as the reductant of AgNO₃ in ethanol with different ratio. The silver layers were estimated using statistical histogram images of FESEM. Silver-coated iron oxide nanohybrids have been used in a broad range of applications, including chemical and biological sensing, due to the broad absorption in the optical region associated with localized surface plasmon resonance.

Keywords: magnetite; silver; polyol; core-shell; magnetic saturation.

1. Introduction

The study of magnetic iron oxide nanoparticles is interesting due to their properties that arise from a finite size, and surface effects that vigorously impacted magnetic properties relative to the bulk for showing remarkable phenomena, such as superparamagnetism [1] and their applications,

in a wide range, such as magnetic fluids hyperthermia [2], magnetic resonance imaging (MRI) [3] and magneto-optics devices [4]. Hybrid nanoparticles that are formed from the combination of two types of nanoparticles are highly regarded in a variety of applications, such as MRI and photothermal therapy [5].

Silver-coated iron oxide nanocrystals have also attracted attention due to their specific characteristics. The decrease in size below the electron mean free path in nanostructures of noble metals gives rise to intense absorption in the optical region associated with localized surface plasmon resonance [6]. Localized surface plasmons have been used in a broad range of applications including chemical and biological sensing [7] and photothermal therapy [8]. Each potential application requires the nanoparticles to have different properties. Silver-coated iron oxide nanohybrids have also been used in a broad range of applications including chemical and biological sensing due to the broad absorption in the optical region associated with localized surface plasmon resonance.

A wide variety of methods have been used to synthesize magnetite nanoparticles, such as co-precipitation method [9], sonochemical [10], liquid polyols [11] and so on. The mechanism of polyol reaction is still under study. Ethylene glycol is a good reducing agent with a relatively high boiling point, and has been widely used in the polyol process as both reductant and solvent to provide monodispersed fine metal, or metal oxide nanoparticles [12]. It has been discovered that the reduction is based on the decomposition of the ethylene glycol and its conversion to acetaldehyde [13]. The temperature is a dominant factor that influences the reducing potential of a polyol compound, rupture and creation of the chemical bond, and diffusion [14]. Sodium acetate is used as a base to maintain a relatively constant pH at around 6.8 during reaction, and as an electrostatic stabilizer to prevent particle agglomeration. It is also an assistant to the ethylene glycol-mediated reduction of FeCl_3 to Fe_3O_4 . It has been reported that polyethylene glycol (PEG) with a uniform and ordered chain structure is easily absorbed at the surface of a metal oxide colloid [15], and acts as a dispersion stabilizer. When the surface of the colloid adsorbs this type of polymer, the activities of the colloid greatly decrease, and the growth rate of certain facets in some of the colloids will be confined [16]. By using PEG as a surfactant, we prevented particle growth, decreased interparticle interactions, and controlled the morphology.

This paper reports modification on the synthesis and characterization of core-shell nanoparticles with a magnetite core and a silver shell by varying the concentration ratio of the reduction agent to deposit of silver on magnetite.

2. Experimental Procedures

The chemical reagents used in this work are ferric chloride 6 hydrate ($\text{FeCl}_3 \cdot 6\text{H}_2\text{O}$), silver nitrate (AgNO_3), sodium acetate, butylamine (99%), polyethylene glycol (MW ~ 3000 Da). All reagents were of analytical grade from Merck and were used without further purification.

The spherical-shaped magnetite nanoparticles have been prepared by using the methods of Deng *et al.* [17] and Kim *et al.* [18]. $\text{FeCl}_3 \cdot 6\text{H}_2\text{O}$ (1.35 g, 5 mmol) was dissolved in ethylene glycol (40 mL) in an ultrasonic bath to form a clear solution. The pH of the solution was acidic. Then sodium acetate (3.7 g, 45 mmol) and polyethylene glycol (1.0 g, 0.05 mmol) were added dropwise to the solution while stirring for 30 min. Then the acquired red precursor refluxed at 190°C for 16 h. After being cooled down to room temperature, the acquired black products were washed several times with ethanol and then dried at 80°C for 8 h. These black products are magnetite. To deposit silver on the magnetite particles, initially, 4 mM ethanolic silvering solution was prepared [Kim, 2010 #10], then 3 mg Fe_3O_4 nanoparticles were dispersed in 30 mL of this solution in a polypropylene container by using an ultrasonic bath. The polypropylene container was used to avoid non-specific silvering of the reaction vessel. At the end, silver coating was achieved by adding butylamine as a weak reductant of AgNO_3 in ethanol. The molar ratios of the ethanolic silvering solution to butylamine were changed as 1:0.5, 1:1 and 1:2, and nominated as S1, S2 and S3, respectively. The resultant solution was incubated for 45 min at 50°C in an ultrasonic bath. After being rinsed with ethanol, the obtained product was redispersed in ethanol under sonication for 5 min.

3. Results and Discussion

Figure 1 shows the FTIR spectra of Fe_3O_4 and S1 core-shell nanospheres.

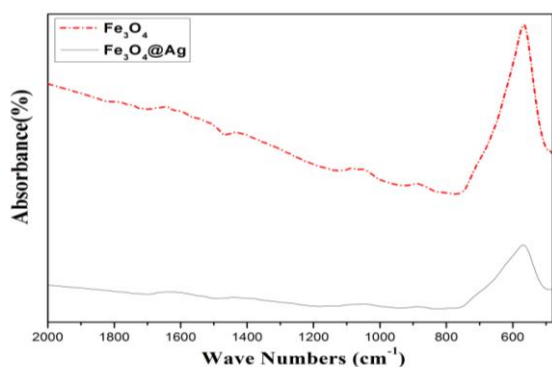


Fig. 1. Fourier transform infrared spectra of Fe_3O_4 and S1 core-shell nanospheres

Infrared studies indicated the presence of a strong absorption line in both coated and pure magnetite located at 567 cm^{-1} which was attributed to the stretching vibration of Fe-O in tetrahedral sites. The band at 1600 cm^{-1} and the broad, intense band observed at $3000\text{--}3500\text{ cm}^{-1}$ (with the maximum at 3400 cm^{-1}) are assigned to the bending of the H-O-H molecules and the O-H stretching vibration, respectively. The peaks at 888 cm^{-1} and 1433 cm^{-1} are attributed to the rocking CH_3 and the bending -C-H vibrations, which show the existence of polyethylene glycol. Additionally, the new absorption peaks at 800 cm^{-1} and 1260 cm^{-1} are assigned to the bending of N-H and C-N of butylamine, respectively, that demonstrates there are some butylamine residues present in the core-shell nanospheres. Due to silver being a metal element, no specific signals are found in the Fourier transform infrared spectroscopy spectrum.

The formation of Fe_3O_4 was confirmed by X-ray diffraction (XRD), and is shown in Figure 2. The X-ray diffraction pattern of as-prepared magnetite shows reflection planes (111), (220), (311), (222), (400), (422), (511) and (440) which were indexed in the $\text{Fd}_3\text{m-O}_h$ ⁷ space group (no. 227) corresponding to a spinel cubic structure, and the XRD spectrum shows no traces of other phases. After

reduction of silver ions, the resulting XRD pattern of the products is shown in Figure 2. As silver is deposited on the surface of magnetite, an additional four diffraction peaks are observed at 38.1 , 44.3 , 64.4 and 77.4 , corresponding to (111), (200), (220) and (311) planes of silver, respectively, with face-centered cubic structure. As well as the characteristic diffraction peaks of Fe_3O_4 , reflections can also be observed in Figure 2.

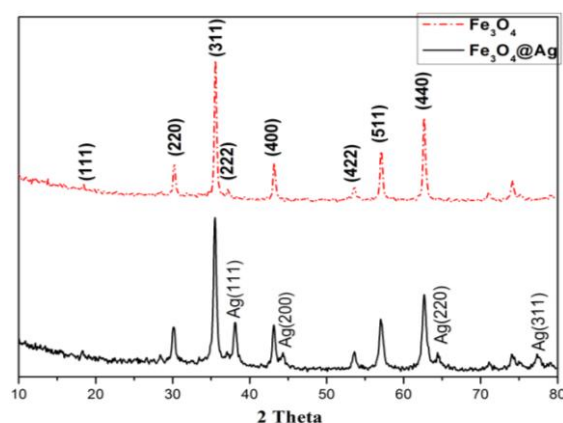


Fig. 2. X-ray diffraction patterns of Fe_3O_4 and S1 core-shell nanospheres

The average size of the grain was determined by applying the Debye-Scherrer equation to the high *intense* peak. The lattice constant of the cubic crystal was computed using the d-spacing values and the respective (hkl) parameters, or directly by:

$$\frac{\sin^2 \theta}{h^2 + k^2 + l^2} = \frac{\lambda^2}{4a^2} \quad (1)$$

but since by increasing θ_{hkl} the lattice constant error decreases, the average lattice constant was determined by applying the above equation to two higher θ_{hkl} values. The results are given in Table 1.

Table 1. Structure properties of Fe_3O_4 and $\text{Fe}_3\text{O}_4@Ag$ core-shell nanospheres

Sample	molar ratios of ethanolic silvering solution: butylamine:and	Lattice strain (%)	Lattice constant (nm)	Particle size (nm)
Fe_3O_4	Fe_3O_4	-	0.385	14
$\text{Fe}_3\text{O}_4@Ag1$	Ag	1:0.5	0.483	28
$\text{Fe}_3\text{O}_4@Ag2$	Ag	1:1	0.474	28
$\text{Fe}_3\text{O}_4@Ag3$	Ag	1:2	0.450	28

The scanning electron microscope shows clusters of fine particles clinging together, and the aggregates are spherical in shape. A statistical histogram shows that the mean diameter of the Fe_3O_4 particles is about 73 nm, as shown in Figure 3a. The agglomerated clusters of particles are due to the magnetostatic coupling between the particles. A statistical histogram of the fine particles on the surface of the powders shows that the

primary particle size is about 16 nm in dimension.

After reduction of silver ions on the surface of magnetite, the smooth surface of the obtained nanocomposites is clearly visible in Figure 4. The approximated silver layers were estimated using statistical histogram images, 3.5, 9 and 11 nm for S1, S2 and S3, respectively.

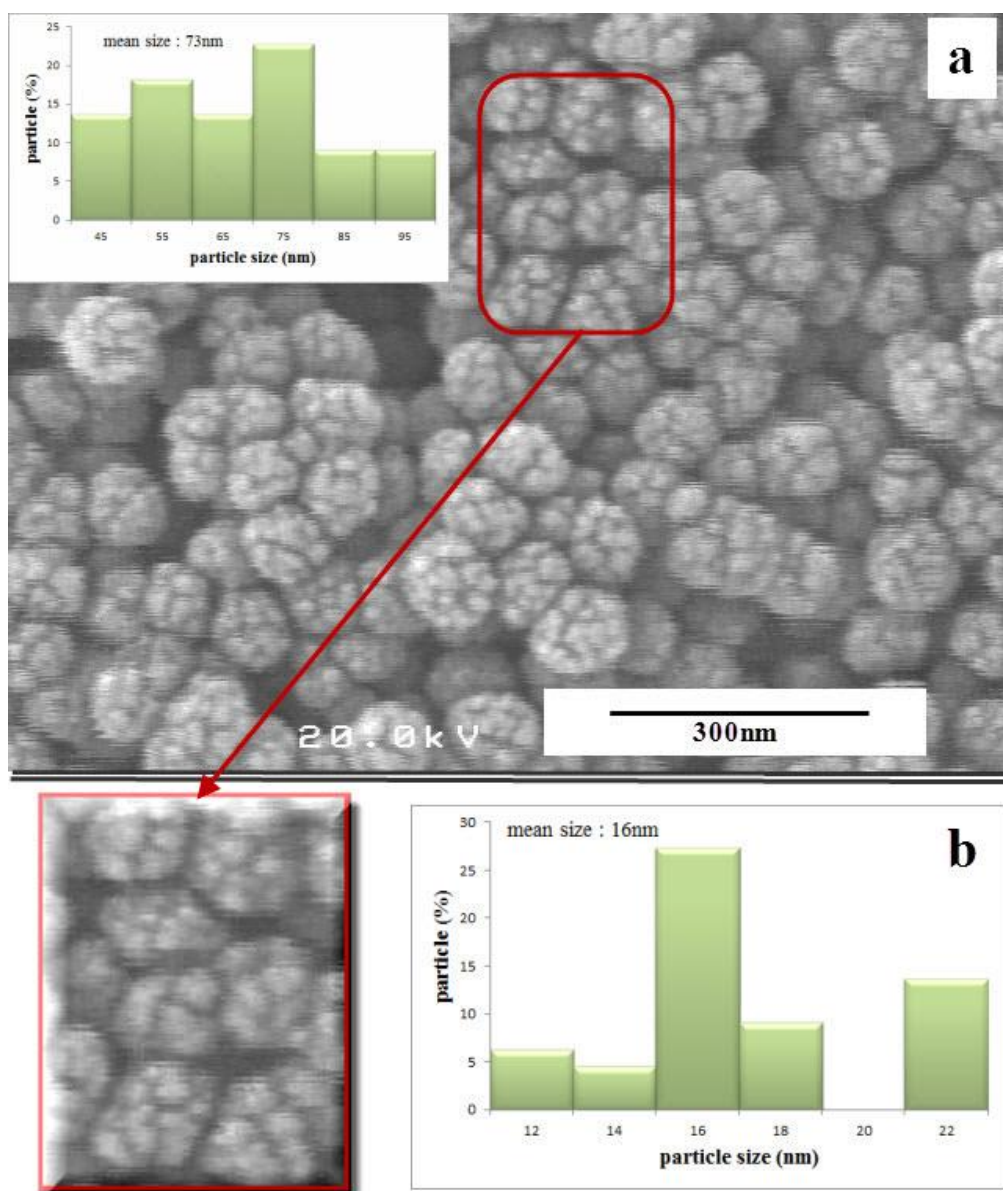


Fig. 3. a) Field emission scanning electron microscope and statistical histogram images of as-prepared Fe_3O_4 nanoparticles synthesized by polyol method, b) the fine particles on the surface of the powders

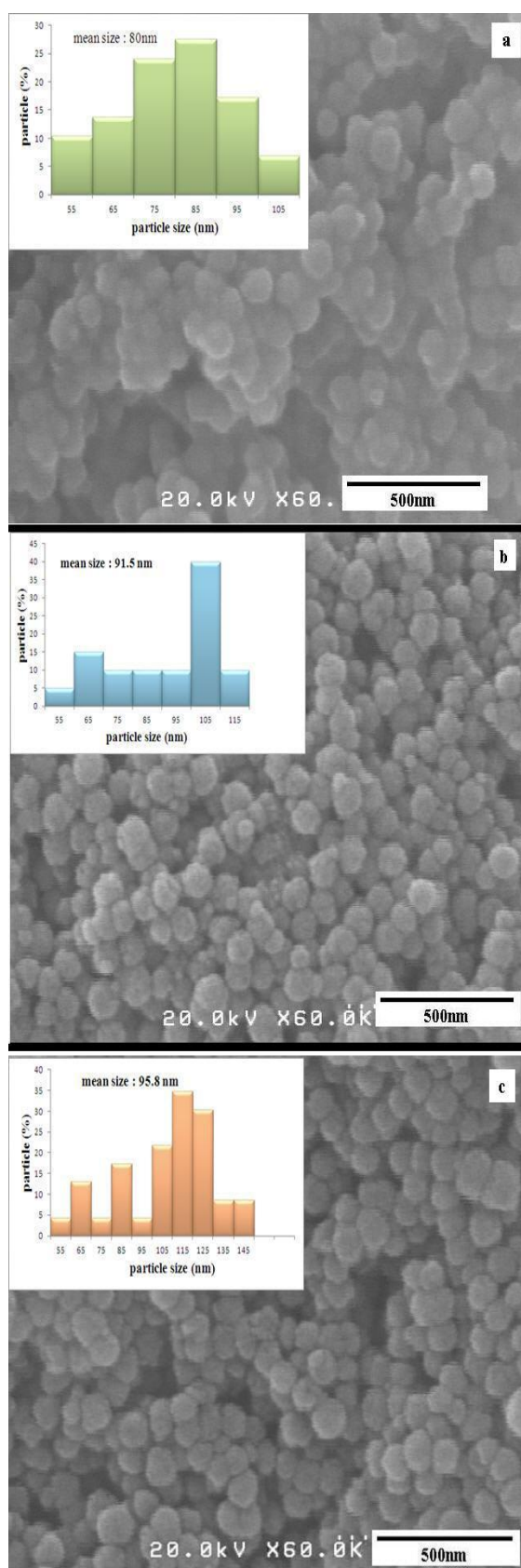


Fig. 4. Field emission scanning electron microscope and statistical histogram images of (a) S1, (b) S2, (c) S3

Magnetic properties of nanoparticles were characterized using vibrating sample magnetometer (VSM with a maximal applied field of 10 kOe. Figure 5 shows the magnetic hysteresis loops of the nanoparticles at room temperature. Saturation magnetization (M_s), coercive field (H_c), and reduced remanent magnetization (M_r/M_s) are given in Table 2.

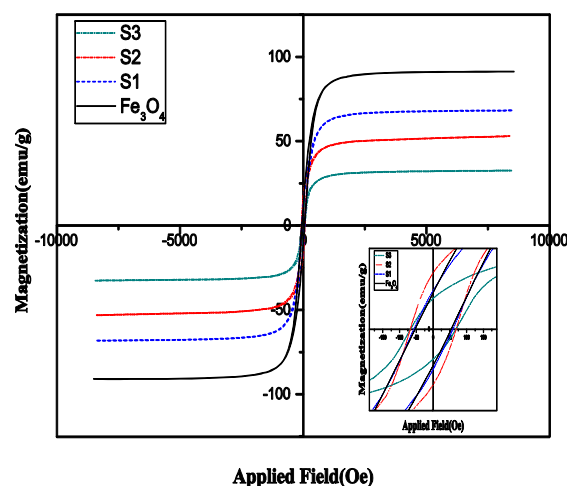


Fig. 5. Hysteresis loops of Fe_3O_4 and $Fe_3O_4@Ag$ core-shell nanospheres

Table 2. magnetic properties of Fe_3O_4 and $Fe_3O_4@Ag$ core-shell nanospheres

Sample	Coercivity (Oe)	M_s (emu/g)	M_r (emu/g)	M_r/M_s
Fe_3O_4	53	91	11	0.12
$Fe_3O_4@Ag1$	57	68	11	0.17
$Fe_3O_4@Ag2$	68	53	17	0.33
$Fe_3O_4@Ag3$	67	32	9	0.29

The magnetic saturation value was 91 emu/g for Fe_3O_4 that was similar to the saturation magnetization value of bulk magnetite. It is easy to infer that the evolution behaviors of M_s and M_r are highly dependent on the growth of nanoparticles, because both the changes of M_s and M_r are in association with the average crystallite size, but here the high saturation magnetization that can be attributed to the very thin dead layers have been observed in transmission electron microscopy (TEM) histogram. The reduced remanence magnetization (the ratio of the remanence (M_r) to the saturation magnetization (M_s)) shows the expected value for random assemblies of single-domain

nanoparticles with magnetostatic coupling. By using polyethylene glycol as a surfactant to separate and restrict the growth of the particles, magnetostatic interactions are dominated in agreement with the remanence ratio analysis. The magnetic saturation values were decreased while the molar ratio of butylamine was increased. It corresponds with increased diamagnetic silver nanoparticles distributed on the surface of magnetite. The coercivity of the magnetite and the Fe₃O₄@Ag core-shell nanoparticles were around 50 Oe. The Ag shell appeared to have no significant effect on the coercivity of the magnetite.

4. Conclusion

In summary, the polyol reduction technique has been used to yield magnetite nanosphere with the saturation magnetization as high as a value of bulk (80 nm diameter) as well as low coercivity (50 Oe). This can be due to the nanoparticles being in the single-domain region agglomerate, and separated by polyethylene glycol, that enhanced the stability of its magnetic properties. Then silver shell was coated on the magnetite nanoparticles by using butylamine as a weak reductant. The remaining magnetization was, nonetheless, strong enough, so that it could be expected to apply this composite to magnetic separation application, functional device assemblies, and MRI through further research and development.

References

- [1].1.Mikhaylova, M., et al., Superparamagnetism of magnetite nanoparticles: dependence on surface modification. *Langmuir*, 2004. **20**(6): p. 2472-2477.
- [2].2.Suto, M., et al., Heat dissipation mechanism of magnetite nanoparticles in magnetic fluid hyperthermia. *Journal of Magnetism and Magnetic Materials*, 2009. **321**(10): p. 1493-1496.
- [3].3.Wan, J., et al., Monodisperse water-soluble magnetite nanoparticles prepared by polyol process for high-performance magnetic resonance imaging. *Chemical Communications*, 2007(47): p. 5004-5006.
- [4].4.Jain, P.K., et al., Surface plasmon resonance enhanced magneto-optics (SuPREMO): Faraday rotation enhancement in gold-coated iron oxide nanocrystals. *Nano letters*, 2009. **9**(4): p. 1644-1650.
- [5].5.Ji, X., et al., Bifunctional gold nanoshells with a superparamagnetic iron oxide-silica core suitable for both MR imaging and photothermal therapy. *The Journal of Physical Chemistry C*, 2007. **111**(17): p. 6245-6251.
- [6].6.Bohren, C.F. and D.R. Huffman, Absorption and scattering of light by small particles. 2008: Wiley-Vch.
- [7].7.Saha, K., et al., Gold nanoparticles in chemical and biological sensing. *Chemical reviews*, 2012. **112**(5): p. 2739-2779.
- [8].8.Huang, X., et al., Plasmonic photothermal therapy (PPTT) using gold nanoparticles. *Lasers in medical science*, 2008. **23**(3): p. 217-228.
- [9].9.Valenzuela, R., et al., Influence of stirring velocity on the synthesis of magnetite nanoparticles (Fe₃O₄) by the co-precipitation method. *Journal of Alloys and Compounds*, 2009. **488**(1): p. 227-231.
- [10].10.Hee Kim, E., et al., Synthesis of ferrofluid with magnetic nanoparticles by sonochemical method for MRI contrast agent. *Journal of Magnetism and Magnetic Materials*, 2005. **289**(0): p. 328-330.
- [11].11.Cai, W. and J. Wan, Facile synthesis of superparamagnetic magnetite nanoparticles in liquid polyols. *Journal of Colloid and Interface Science*, 2007. **305**(2): p. 366-370.
- [12].12.Cao, S.-W., Y.-J. Zhu, and J. Chang, Fe₃O₄ polyhedral nanoparticles with a high magnetization synthesized in mixed solvent ethylene glycol-water system. *New Journal of Chemistry*, 2008. **32**(9): p. 1526-1530.
- [13].13.Drake, N.L. and T.B. Smith, THE DECOMPOSITION OF ETHYLENE GLYCOL IN THE PRESENCE OF CATALYSTS. I. VANADIUM PENTOXIDE AS CATALYST. *Journal of the American Chemical Society*, 1930. **52**(11): p. 4558-4566.
- [14].14.Ding, T., et al., Sonochemical synthesis and characterizations of monodispersed PbSe nanocrystals in polymer solvent. *journal of crystal growth*, 2002. **235**(1): p. 517-522.
- [15].15.Dobryszycski, J. and S. Bialozor, On some organic inhibitors of zinc corrosion in alkaline media. *Corrosion science*, 2001. **43**(7): p. 1309-1319.

- [16]. 16. Bognitzki, M., et al., Polymer, metal, and hybrid nano-and mesotubes by coating degradable polymer template fibers (TUFT process). *Advanced Materials*, 2000. **12**(9): p. 637-640.
- [17]. 17. Deng, H., et al., Monodisperse Magnetic Single-Crystal Ferrite Microspheres. *Angewandte Chemie*, 2005. **117**(18): p. 2842-2845.
- [18]. 18. Kim, K., et al., Silanization of Ag-Deposited Magnetite Particles: An Efficient Route to Fabricate Magnetic Nanoparticle-Based Raman Barcode Materials. *ACS Applied Materials & Interfaces*, 2010. **2**(7): p. 1872-1878.